

# 7. Experimental set-up

## 7.1. The electrochemical etching system

Along the last decade, the interest of our research group has been focused on NTD application in several fields of investigation such as cosmic rays, interaction of heavy ions with matter, neutron dosimetry and radon monitoring. In the neutron and radon fields, electrochemically etched CR-39 and Makrofol detectors are respectively used. The electrochemical etching system developed in our laboratory for Makrofol detectors (see Figure 7.1) consists of:

1. An alternative high voltage/frequency generator with a nominal variation ranges, from 300 V to 2500 V and from 2.5 kHz to 5 kHz, respectively.
2. A frequency-meter (Tektronix CFC250)<sup>1</sup> with a digital visualising that is connected to a selector with 3 positions for the electric parameter reading. The value given by the frequency-meter corresponds directly to the ECE frequency in Hz if the selector is at the position 2, is 4 times the ECE voltage in V if the selector is at the position 3, and is 100 times the ECE current in mA if the selector is at the position 1.
3. An electric thermo-controlled stove, of 0.1 °C precision, equipped with an air circulating fan to keep the temperature stable and homogeneous during the chemical and/or electrochemical etching. The temperature of this stove is regulated automatically reaching a maximum value of 200 °C.
4. A security device to let the generator switch-off when occurring an electrical short-circuit or when opening the stove door.
5. A modular system of etching cell (Figure 7.2) for processing simultaneously up to 20 detectors. It consists of 11 plates (16.5 cm long, 11 cm high and 1.2 cm thick) and 20 transparent rubber foils (16.5 cm long, 11 cm high and 0.2 cm thick), both fabricated with PVC plastic.

---

<sup>1</sup>Manufactured by Tektronix Inc., USA.

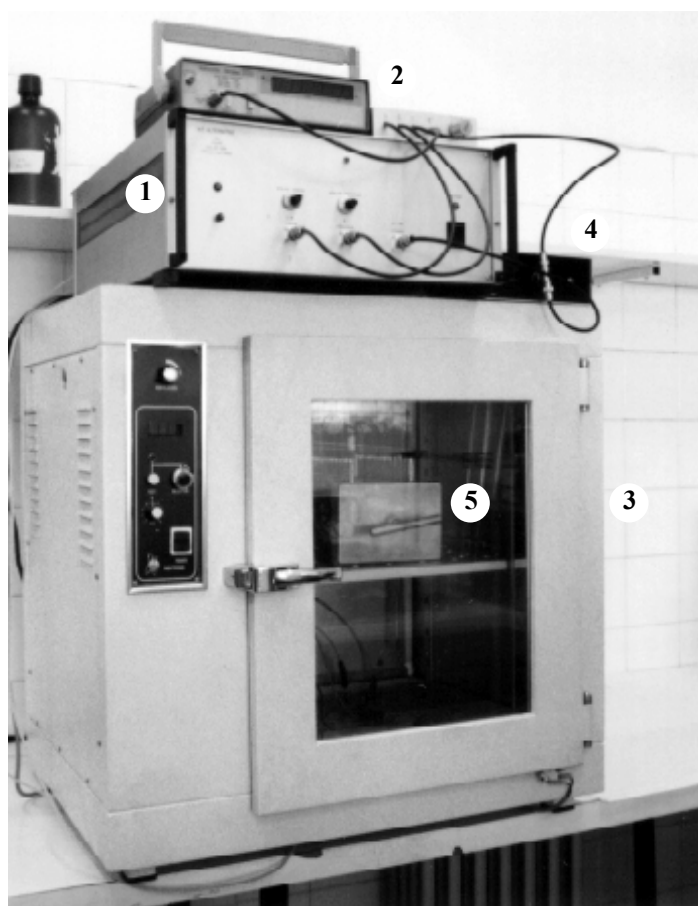


Figure 7.1. Elements of the electrochemical etching equipment: (1) the high alternative voltage/frequency generator, (2) the digital frequency-meter with a frequency-voltage-current selector, (3) the electric stove, (4) the security device, and (5) the modular etching cell system.

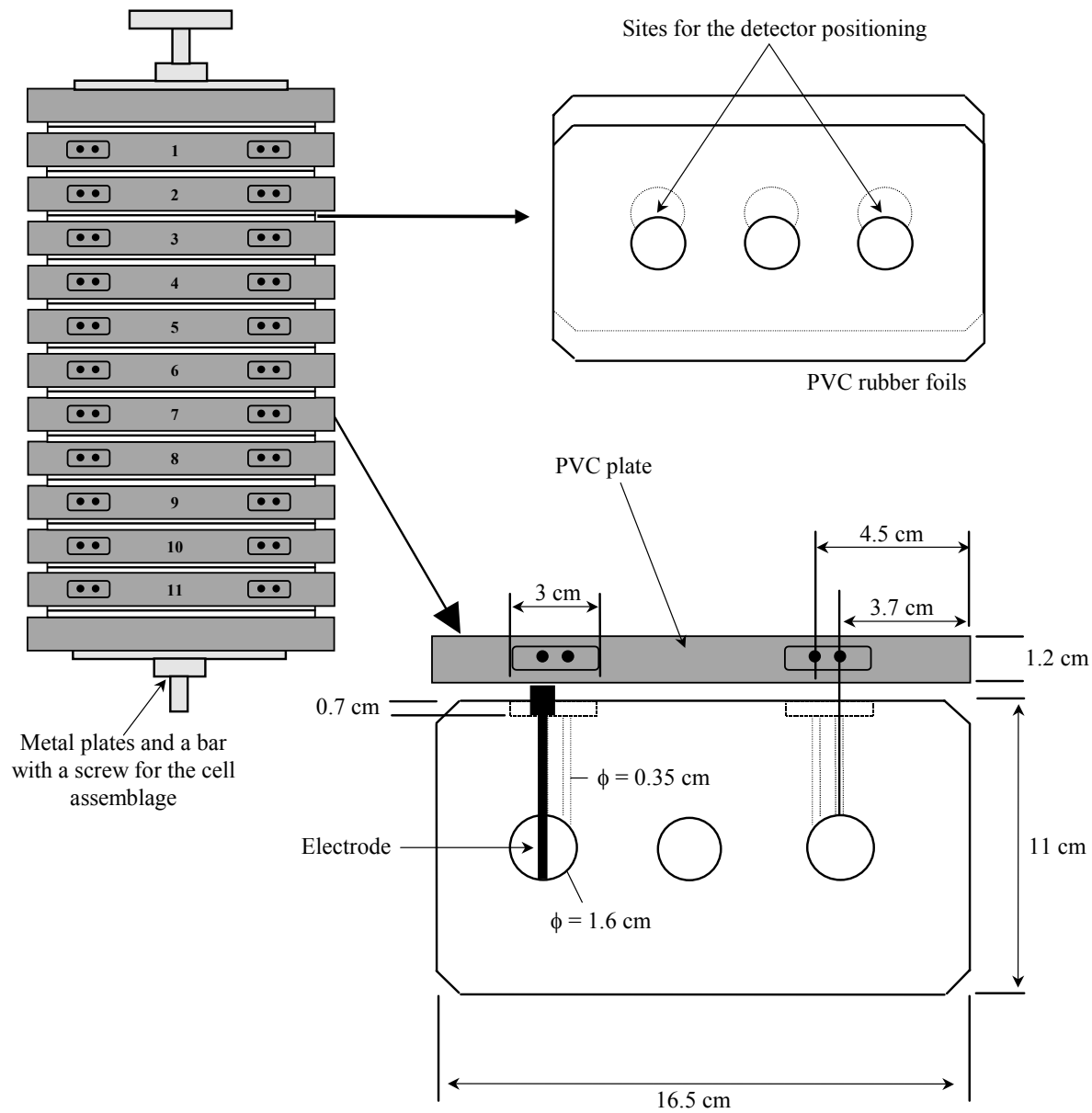


Figure 7.2. Schematic illustration of the modular cell system used for electrochemical etching of the Makrofol detectors.

As shown in Figure 7.2, the PVC plates of the etching cells are sandwiched together with two rubber foils being the Makrofol detectors inside these last. The conjunct is pressed by means of two stainless steel plates and a bar with a screw. Each PVC plate is perforated by 4 holes of 0.3 diameter in its upper vertical direction: two interior holes to inject the electrolyte dissolutions and two exterior holes to introduce the electrodes to be connected to the AC generator. In the transversal plan of the PVC plates, there are two lateral cavities of 1.6 cm diameter and 1.2 cm long, which are interconnected with the 4 holes, to put the detectors and a central cavity with the same dimensions that lets the cell closing by the bar and the screw. The rubber foils have also three 1.6 cm diameter orifices with the same finality as the PVC plate cavities. The etchant (the KOH dissolution mixed with alcohol) is injected inside the two lateral cavities of the even PVC plates of the modular cell system in direct contact with the sensible side of the Makrofol detectors to be etched. In the lateral cavities of the odd PVC plates, we add a dissolution of 0.25 N KOH to close the electric circuit. In this manner, the electrodes of the plates with the etchant are in parallel position to those of the plates with the other electrolyte dissolution.

The methodology used for the preparation of KOH dissolution with a given molarity is explained in Amgarou (1997). Before pre-etching, the etchant and the modular cell system are pre-heated separately for more than 4 h within the stove at the required temperature to insure a good stabilisation of this last. The pre-etching is initialised as soon as the etchant takes contact with the detectors.

## 7.2. The track counting system

Automation of the track reading process is highly desirable to reduce errors due to human appreciation and to improve NTD reproducibility. Since 1991, we have used a semi-automatic track counting system able to evaluate both chemical and electrochemical tracks in, practically, any type of NTDs (Amgarou et al., 2001a). In the case of electrochemically etched Makrofol detectors, this system employs a photo video camera (Sony PHV-A7E)<sup>2</sup>, working in the transmission mode, connected to a frame-grabber board (Matrox PIP 1024B)<sup>3</sup> of a limited spatial resolution of  $512 \times 512$  pixels. Although it offers quite successfully results, its response deviates from linearity at high track density above  $1000 \text{ cm}^{-2}$ . Furthermore, the track analysis software used is obsolete and is executable only under MS-DOS requiring the use of an external TV-monitor for visual control.

At the present, seeing the latter advances and innovations that have occurred in digital technology field, one of the possible and less expensive improvement of the existing

---

<sup>2</sup>Manufactured by Sony Corporation, Japan.

<sup>3</sup>Manufactured by Matrox Electronic Systems Ltd., Canada.

semi-automatic system can be carried out by means of any of the commercially available digital TV-graphic cards. Of these, the 24-bit Hauppauge WinTV<sup>4</sup> card was selected as being convenient to scan the detector images with a sufficient quality and it was incorporated into a 300 MHz PC Pentium with 64 Mbytes of RAM and 3.2 Gbytes hard drive. By using the control software of the WinTV board, the detector image of the photo video camera can be captured with a spatial resolution up to  $1600 \times 1200$  pixels and can be stored in the specified directory under any of the standard digital file formats including tiff, bmp, jpg, gif, etc. On the other hand, this software can also adjust the values of the image brightness, contrast, saturation and hue. These adjustments in conjunction with the IRIS selector<sup>5</sup> of the photo video camera permit the optimisation of the track recognition and the discrimination of stains, scratches and other unwanted inhomogeneities on the detector surface.

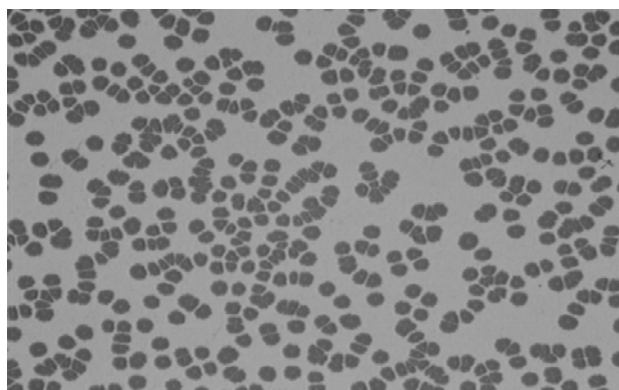


Figure 7.3. A typical image of electrochemically etched Makrofol detectors as captured by the new semi-automatic system using an optical field area of  $8.4 \times 6.3 \text{ mm}^2$ .

Figure 7.3 presents a typical image of the electrochemically etched Makrofol detectors as captured by the new semi-automatic system using an optical field of  $8.4 \times 6.3 \text{ mm}^2$ . In this figure, we observe that the electrochemically etched tracks are genuine objects with specific properties such as size, shape, position and optical density. The analysis software chosen to extract the vital information of these tracks is a public domain Java image processing program, developed at the National Institute of Health (NIH) of USA, called ImageJ<sup>6</sup>. This software and that of the WinTV card are supported by Windows 95 (or higher) ensuring a suitable interface with the user. The main characteristics of the ImageJ program are the following:

---

<sup>4</sup>Manufactured by Hauppauge Computer Works Inc., USA.

<sup>5</sup>An adjustable button that controls the amount of the light transmitted to the camera sensor.

<sup>6</sup>Freely available at: <http://rsb.info.nih.gov/ij>.

1. It supports all the standard functions for the image enhancement, noise reduction, background subtraction, edge detection and feature identification.
2. Its functionality can be expanded via easy-to-use Java plug-in customs to solve almost any problem of image analysing or complex data representation.
3. It can display simultaneously a large number of additional windows of detector images or graphs, limited only by the available computer memory.
4. It offers the possibility of a parametric calibration to any unit of reference (spatial, density or grey-level) in order to give a real approach of the measured quantities.

Figure 7.4 shows an illustration of the procedures used by the ImageJ program to evaluate electrochemically etched Makrofol detectors. For track characterisation and classification, the most adequate parameter is the change of the light density from light to dark on the boundary of each track. Consequently, it is sufficient to map the detector image onto 8 bits per pixel allowing only 256 discrete grey-level values that range from 0 for pure black pixel to 255 for pure white pixel. The lower observable limit of the electrochemical etched tracks is of about  $12.5 \mu\text{m}$  in diameter. By defining automatically the lower and upper grey-level thresholds, the program is able to isolate all the detector tracks even in high background. Each identified track is marked in red on the corresponding image screen. The results of its morphology (area, perimeter, grey-level,  $xy$  coordinates, etc.) measurements are listed in the program menu dialog box and can be exported as a tab-delimited text file to be used latter on.

To test the performance of this new semi-automatic system, we have compared its response to that of manual track counting. This last was carried out by way of a microfiche reader VALIANT-LP<sup>7</sup> of  $31\times$  magnification, using a grid surface of  $8.0 \times 6.0 \text{ mm}^2$ . In Figure 7.5, we present the comparative study of both systems to evaluate track densities on electrochemically etched Makrofol detectors after being exposed to different  $^{222}\text{Rn}$  exposures. Also shown in this figure are the results of track density measurements of the same detectors using the old semi-automatic reader, whose behaviour does not differ from that reported in a previous study of our group (Amgarou et al., 2001a). In contrast to the old system, the track densities found when using the WinTV card and the ImageJ program are consistent with those obtained with the manual counting showing no deviation from the linearity curve,  $f(x) = x$ , up to a track density of  $1000 \text{ cm}^{-2}$ . The error of track underestimation due to overlapping effect is significant only for track densities higher than  $1500 \text{ cm}^{-2}$ , where the fraction of track lost never exceeds the 10% of tracks counted by

---

<sup>7</sup>Manufactured by Realist Micrographic Systems, USA.

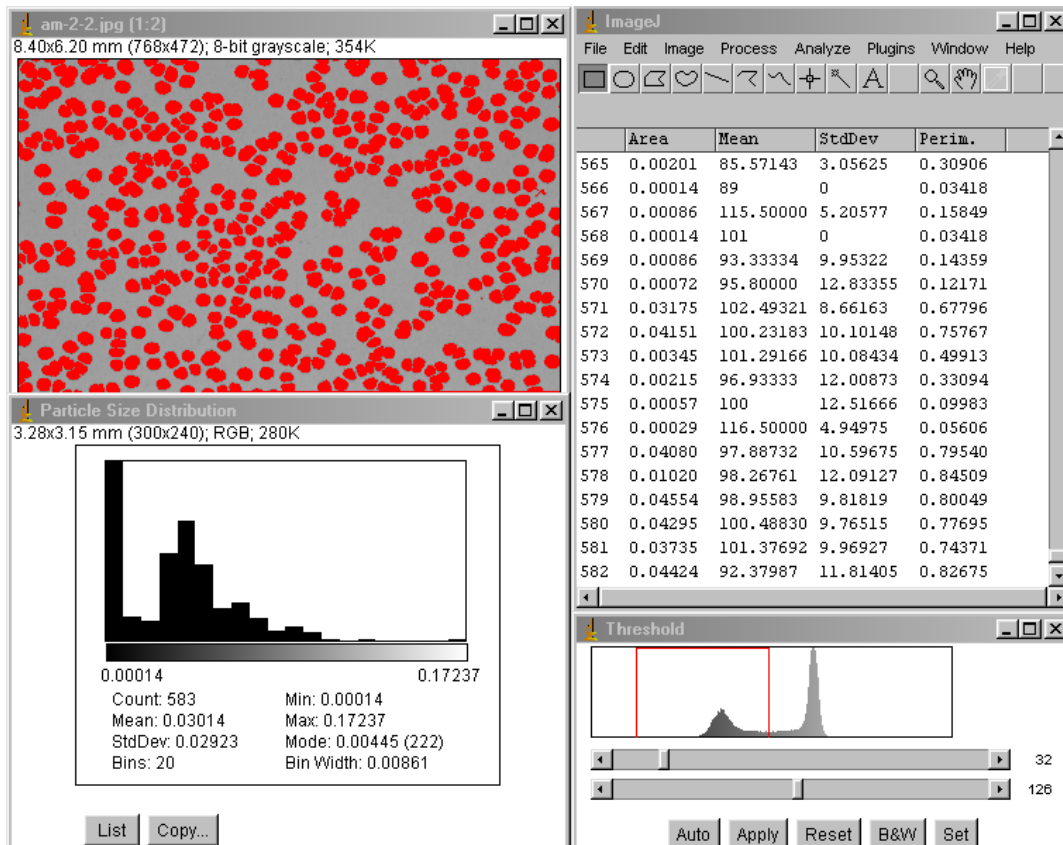


Figure 7.4. Illustration of the procedures used by the ImageJ program to evaluate electrochemically etched Makrofol detectors. By defining automatically the lower and upper grey-level thresholds (see the bottom right dialog box), the tracks are isolated and marked in red on the corresponding image screen (high left dialog box). The results of track morphology measurements are listed in the program menu window (high right dialog box). If required, additional histogram of the track area distribution can also be displayed (bottom left dialog box).

the microfiche reader, at least, up to a track density of  $2000 \text{ cm}^{-2}$ . This result means a remarkable improvement of our semi-automatic track counting system.

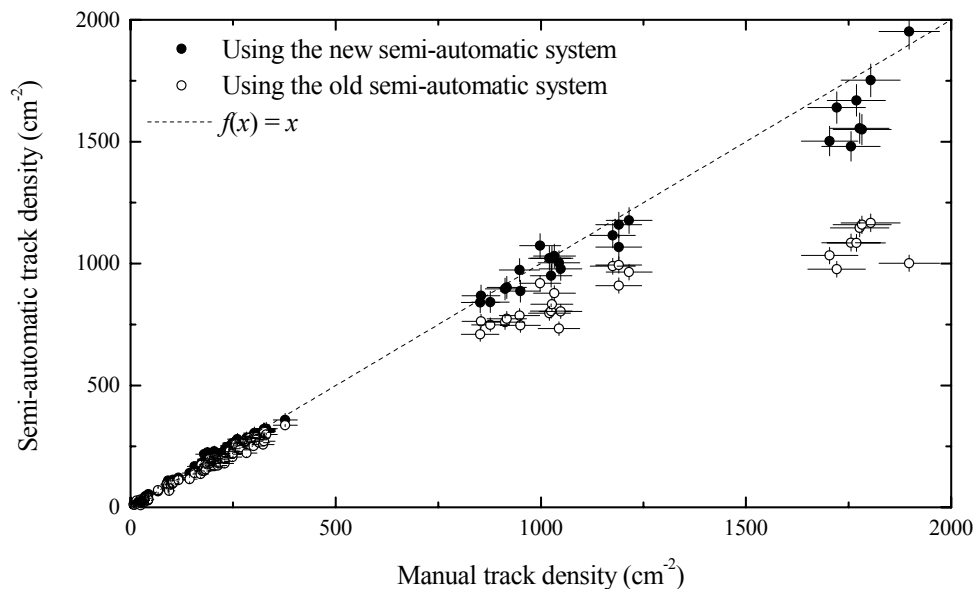


Figure 7.5. Response of the new and the old semi-automatic systems for track evaluation of electrochemically etched Makrofol detectors with respect to the manual counting. The error bars correspond to one standard deviation.

### 7.3. The set-up of a small exposure chamber

The idea of constructing a small exposure chamber was originated as a consequence of the wide experience of our group in this field as well as from the fact that currently there is not any facility in Spain allowing the exposure to both  $^{222}\text{Rn}$  and  $^{220}\text{Rn}$ <sup>8</sup>. In order to enable the fulfillment of this project, the conception and the realisation of this chamber is designed to be done into three phases:

1. The first phase consists on performing a set of pilot experiments using a  $^{222}\text{Rn}$  source in order to find the optimum geometry of the chamber and the disposition of  $^{222}\text{Rn}$

---

<sup>8</sup>At the present time, the Institute of Energetic Techniques (INTE) of Barcelona maintains a sophisticated  $20 \text{ m}^3$  walk-in exposure chamber (Vargas, 2000), which is licensed to be the national reference laboratory. However, this facility performs measurements only in pure  $^{222}\text{Rn}$  atmospheres.



source. In this phase, efforts are directed to control the  $^{222}\text{Rn}$  concentration, which is intended to be monitored continuously together with the environmental conditions (temperature, atmospheric pressure and relative humidity). The size of the chamber must be as small as possible to enhance the concentration homogeneity inside it, especially for  $^{220}\text{Rn}$  gas, and to allow changes in the exposure conditions on relatively small time scales.

2. In the second phase, the  $^{222}\text{Rn}$  progeny concentration within the chamber should be controlled and measured, in order to obtain the subsequent equilibrium factor and the potential  $\alpha$ -energy concentration, by incorporating an aerosol generator and a continuous WL (Working Level) monitor, respectively. Mechanisms of temperature and relative humidity control will also be incorporated in this phase.
3. As a final step, in the last phase, a  $^{220}\text{Rn}$  source will be incorporated to be used independently or simultaneously with the  $^{222}\text{Rn}$  source to analyse its contribution to the detector reading.

The set up of the first phase was within the objectives of this work. Figure 7.6 illustrates the experimental arrangement for the  $^{222}\text{Rn}$  facility test developed. The prototype exposure chamber consists of two parts: an exposure volume (110 L) and a  $^{222}\text{Rn}$  gas generator. The exposure volume is an air-tight cubic box ( $50 \times 50 \times 50 \text{ cm}^3$ ) made of plastic methacrylate with 1 cm thickness. The internal housing of the plastic box was covered by 0.1 mm brass metal, which being electrically grounded permits to minimise any effect of electrostatic charge on  $^{222}\text{Rn}$  progeny deposition. Two inlet and outlet openings were made in two opposite lateral sides of the plastic box to supply/exhaust  $^{222}\text{Rn}$  gas and to take air samples to be measured. Another opening was made in one corner at the top side of the box to let the electronic connection of the weather station sensor (Davis Weatherlink)<sup>9</sup> that gives information about temperature, atmospheric pressure and relative humidity inside the exposure volume. The relative humidity of the exposure chamber can be decreased to low values using silica blue gel as a desiccant agent. At the center in the top side of the box there is a sealed  $40 \times 40 \text{ cm}^2$  access door, which can be opened for putting various equipment or detectors into the exposure volume.

The reference instrument for the concentration measurement, is the portable scintillation cell monitor PRASSI<sup>10</sup>, which is connected to the exposure chamber through a valve and an in-line filter holder. This monitor consists basically of a 1.83 L cell coated with zinc sulfide activated with silver,  $\text{ZnS}(\text{Ag})$ , and coupled to a low-gain-drift photomultiplier. It can operate in continuous measurement as well as in grab-sampling modes and it

---

<sup>9</sup>Manufactured by Davis Instruments, USA.

<sup>10</sup>Manufactured by Silena S.p.A., Italy.

is equipped with an auto-regulated pump that supplies a constant flow rate of  $3 \text{ L min}^{-1}$ . The measurement data can be transferred, from a RS232 serial port, into an ASCII file on a personal computer.  $^{222}\text{Rn}$  is generated from approximately 5 kg of uranium rich ore, pitchblende, which was previously powdered to promote  $^{222}\text{Rn}$  exhalation and packed in small polyethylene bags, each one with 250 g of mass. These bags could be placed at the bottom of the chamber or outside into a flask with a valve. The  $^{222}\text{Rn}$  concentration inside the chamber is controlled by varying the source quantity, i.e., the number of the pitchblende bags. The  $^{222}\text{Rn}$  concentration inside the chamber is controlled by varying the source quantity, i.e., the number of the pitchblende bags. The  $^{222}\text{Rn}$  levels obtained in this way range from  $10 \text{ kBq m}^{-3}$  to  $1.5 \text{ MBq m}^{-3}$ .

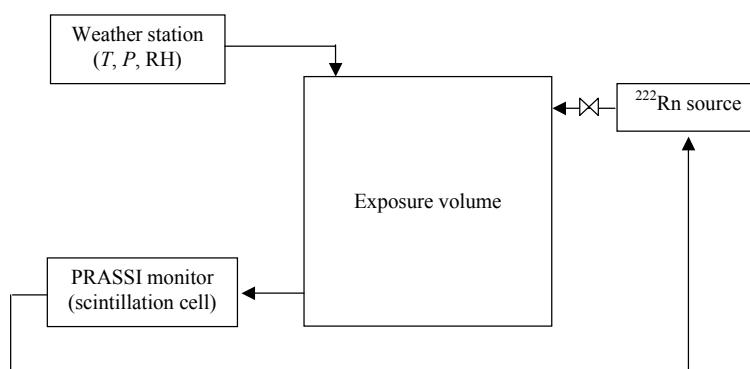


Figure 7.6. Experimental arrangement for the  $^{222}\text{Rn}$  facility test developed in the present work.

The exposure chamber works in the recirculation mode; so that, when the source valve is open, the radioactive gas pass to the exposure volume, then, the PRASSI monitor extracts air from the outlet of the exposure volume — at the constant flow rate said above — and turn it back another time to the  $^{222}\text{Rn}$  source flask. Consequently, a closed air circuit with homogeneous  $^{222}\text{Rn}$  concentration is achieved in a few minutes. The PRASSI monitor measures continuously the  $^{222}\text{Rn}$  concentration with times steps ranging from 15 minutes up to 24 hours. The results of the measurement can be transferred, from a RS232 port, into an ASCII file on a personal computer. All the connections of this circuit are made of plastic hoses. Figure 7.7 gives an example of  $^{222}\text{Rn}$  concentration built-up inside the exposure chamber together with the subsequent environmental conditions as measured by the PRASSI monitor and the weather station, respectively. It is shown in this figure that, during the exposure, the chamber pressure remains constant, the changes in the relative humidity are lower than 2% and the temperature varies only within  $\pm 2 \text{ }^\circ\text{C}$  due to the day-night variation effect.

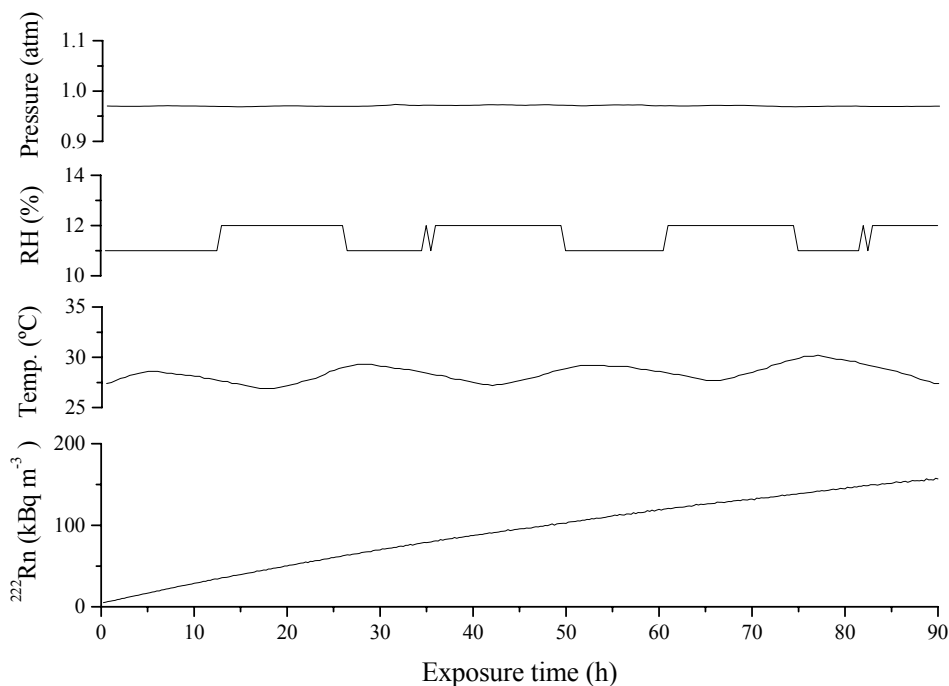


Figure 7.7. An example of  $^{222}\text{Rn}$  concentration built-up inside the exposure chamber together with the subsequent environmental conditions as measured by the Prassi monitor and the weather station, respectively.

#### 7.4. The set-up of a high $\alpha$ -energy irradiator

To well optimise experimentally the Makrofol response, it is necessary to irradiate the detector plates with mono-energetic  $\alpha$ -particles from 2 MeV up to 8 MeV. Irradiation to low energetic  $\alpha$ -particles (below 5.0 MeV) can be made simply with an  $^{241}\text{Am}$  source of  $\sim 3.7$  kBq activity<sup>11</sup> available in our laboratory, while irradiation to high  $\alpha$ -energies suffers from the absence of long-lived standard sources. With this in view, we generate a  $^{212}\text{Bi}/\text{Po}$  source with a sufficient purity by electrostatic precipitation of  $^{216}\text{Po}^+$  ions, formed as a consequence of  $^{220}\text{Rn}$  decay process, on a metallic target disk of 2.9 cm diameter. The  $^{220}\text{Rn}$  exhalation is ensured by means of a small thorium sample, of  $\sim 28$  g mass and  $\sim 37$  kBq activity<sup>12</sup>, within a special air-tight device made of PVC plastic of a cylindrical shape. The deposited  $^{216}\text{Po}^+$  ions decay rapidly to form the  $^{212}\text{Pb}$  which is the most important

<sup>11</sup>As given by the manufacturer.

<sup>12</sup>As given by the manufacturer.

$^{220}\text{Rn}$  daughter due to its relative long half-life. However, as shown in Figure 2.2, since  $^{212}\text{Pb}$  is a  $\beta$ -emitter the only  $\alpha$ -emissions — of energies 6.07 MeV (with a branching ratio of 0.36) and 8.78 MeV (0.64 branching ratio) — come respectively from the subsequent decay products  $^{212}\text{Bi}$  and  $^{212}\text{Po}$ . The considerable difference between the two energies, makes the  $^{212}\text{Bi}/\text{Po}$  source very convenient in determining experimentally the  $\alpha$ -energy window response of, practically, any type of  $\alpha$ -detection system.

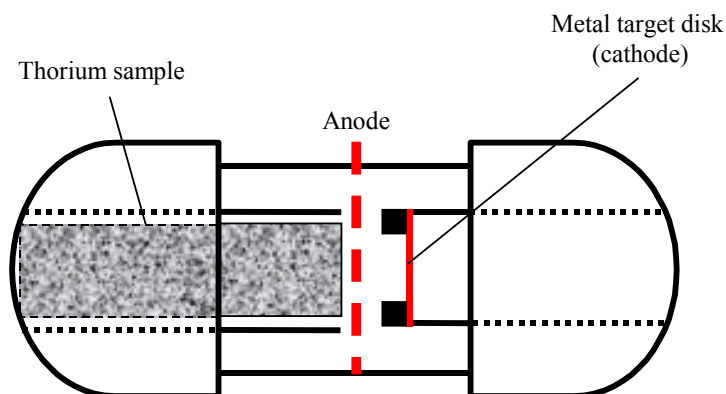


Figure 7.8. Schematic illustration of the device used to generate the  $^{212}\text{Bi}/\text{Po}$  source.

A schematic illustration of the device used to generate the  $^{212}\text{Bi}/\text{Po}$  source is shown in Figure 7.8. The thorium sample and the target disk are placed in opposite sides of the device and are separated by a metallic grid acting as an anode. The  $^{220}\text{Rn}$  gas emanated from the thorium sample and diffuses through the metallic grid; so that, the decay products are electrostatically collected on the target disk that is electrically grounded to close the circuit. Applying a high voltage of  $\sim 500$  V between the anode and the cathode, a saturation total activity of  $\sim 200$  Bq is obtained after a collection time of 20 hours approximately.

Both the  $^{241}\text{Am}$  and the generated  $^{212}\text{Bi}/\text{Po}$  sources are placed in the free air at a given distance faced toward the Makrofol detector to be irradiated. The obtention of any  $\alpha$ -energy of interest, at any time-interval, can be produced by varying only the distance between the source and the detector. Before irradiation, reference measurements of the  $\alpha$ -spectrum are made using a Surface Barrier Detector (SBD) coupled to a multi-channel pulse analyser at the same position as that normally occupied by the Makrofol plates. In Figures 7.9 and 7.10, are presented respectively the  $\alpha$ -spectrums of the  $^{241}\text{Am}$  and  $^{212}\text{Bi}/\text{Po}$  sources measured by the SBD at different source-detector distances. It can be clearly seen in these figures that the energy and the number of incident  $\alpha$ -particles decreases as the distance between the source and the detector increases. The lower peak shown at energies

below 2 MeV for the  $^{212}\text{Bi}/\text{Po}$  source, see Figure 2.2, corresponds to mainly  $\beta$ -emissions of  $^{212}\text{Pb}$ ,  $^{212}\text{Bi}$  and  $^{212}\text{Tl}$  in the  $^{220}\text{Rn}$  chain. This finding were confirmed by using standard  $\gamma$ - and  $\beta$ -sources observing that SBD is sensitive only to  $\beta$ -particles whose spectrum extends down into low energy region ( $< 2$  MeV).

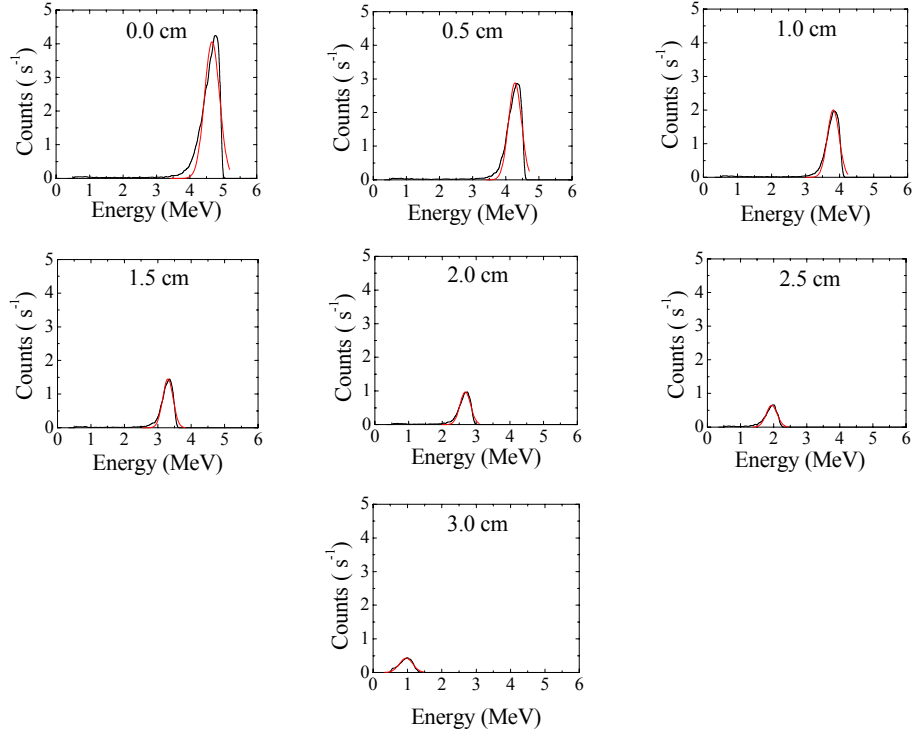


Figure 7.9. Measured  $\alpha$ -spectrum of the  $^{241}\text{Am}$  source by the multichannel pulse analyser at different source-to-detector distances. The peaks of interest have been fitted to a normal distribution.

The maximum distance that we can use for the detector irradiation to  $^{241}\text{Am}$  and  $^{212}\text{Bi}/\text{Po}$  sources are 3.0 cm and 4.5 cm, respectively. The reference energies chosen are reported with one standard deviation in Table 7.1. An apparent disadvantage of this irradiation configuration is the possible spread in  $\alpha$ -energy spectrum, specially at low energies. Nevertheless, according to the data of the Table 7.1,  $\alpha$ -particles, of energy steps of  $\sim 0.5$  MeV in the case of using the  $^{212}\text{Am}$  source and of  $\sim 0.3$  MeV when the  $^{212}\text{Bi}/\text{Po}$  source is used, could be produced between 2.0 MeV and 8.1 MeV with an  $\alpha$ -energy resolution lower than 10%.

The energy-distance curves obtained for both the  $^{241}\text{Am}$  and  $^{212}\text{Bi}/\text{Po}$  sources are shown in Figure 7.11. These curves are useful if we need to irradiate the Makrofol detector at intermediate  $\alpha$ -energies. For a chosen  $\alpha$ -energy, the integral of the reference peak area measured by the SBD is used to calculate the particle fluence at the considered distance. The number of incident  $\alpha$ -particles able to reach the Makrofol detector surface at the moment of irradiation can be estimated, taking into account the half-life (10.64 h) of the  $^{212}\text{Pb}$  and the time elapsed from the SBD reference measurement to the Makrofol detector irradiation. Even though  $\alpha$ -particles of energies below 5 MeV could be also generated by the  $^{212}\text{Bi}$ , this last can not be used for the Makrofol detector irradiation because of its low activity and of the poor resolution of the  $\alpha$ -energies obtained, especially when the source-detector distance is increased.

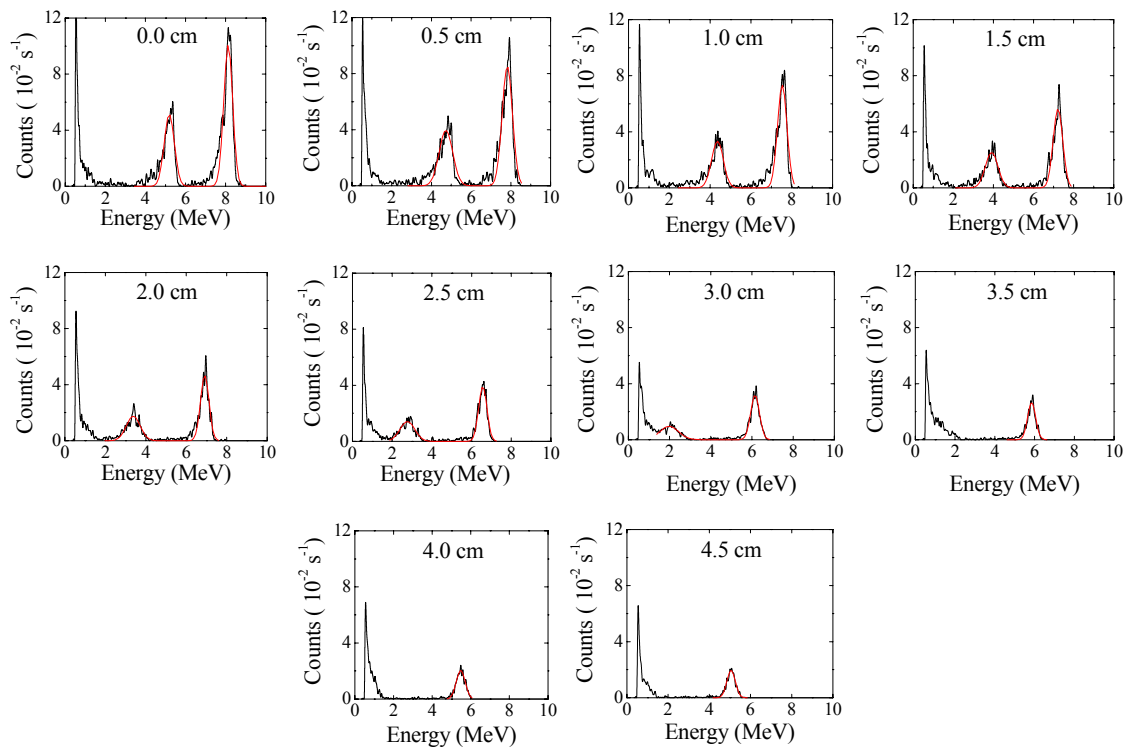


Figure 7.10. Measured  $\alpha$ -spectrum of the  $^{212}\text{Bi}/\text{Po}$  source by the multichannel pulse analyser at different source-to-detector distances. The peaks of interest have been fitted to a normal distribution.

Table 7.1. Reference  $\alpha$ -energies used for the Makrofol detector irradiation.

Distance (cm)	Reference Energy (MeV)		
	$^{241}\text{Am}$ source	$^{212}\text{Bi}$ source	$^{212}\text{Po}$ source
0.0	$4.8 \pm 0.3$	$5.2 \pm 0.3$	$8.1 \pm 0.2$
0.5	$4.4 \pm 0.2$	$4.7 \pm 0.4$	$7.8 \pm 0.3$
1.0	$3.8 \pm 0.2$	$4.4 \pm 0.3$	$7.5 \pm 0.2$
1.5	$3.3 \pm 0.2$	$3.9 \pm 0.3$	$7.2 \pm 0.2$
2.0	$2.7 \pm 0.2$	$3.4 \pm 0.4$	$6.9 \pm 0.2$
2.5	$2.0 \pm 0.2$	$2.8 \pm 0.4$	$6.6 \pm 0.2$
3.0	$1.0 \pm 0.2$	$2.0 \pm 0.5$	$6.2 \pm 0.2$
3.5	—	—	$5.9 \pm 0.2$
4.0	—	—	$5.5 \pm 0.2$
4.5	—	—	$5.1 \pm 0.2$

Uncertainty corresponds to one standard deviation

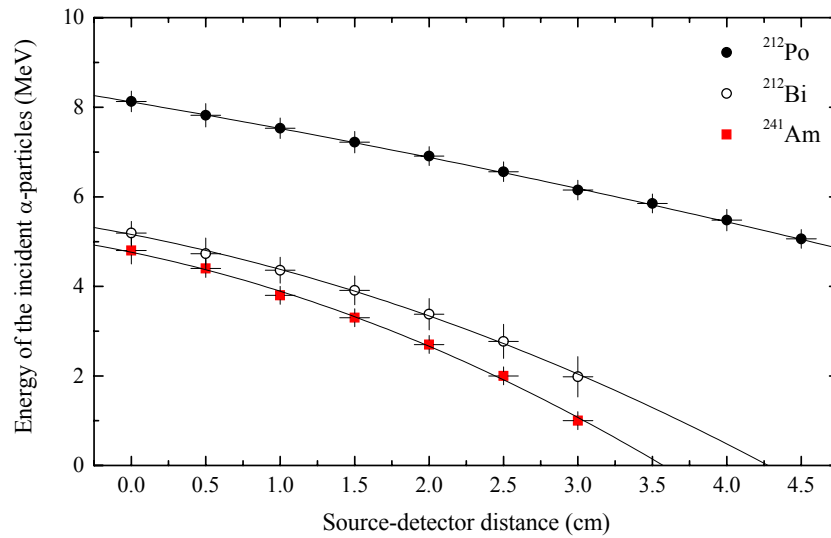


Figure 7.11. Energy-distance curves obtained for both the  $^{241}\text{Am}$  and  $^{212}\text{Bi/Po}$  sources. The error bars correspond to one standard deviation.

